

Available at www.sciencedirect.com

SciVerse ScienceDirect

journal homepage: www.elsevier.com/locate/modo

Active reinforcement of externally imposed folding in amphibians embryonic tissues

Stanislav V. Kremnyov^{*}, Tatyana G. Troshina, Lev V. Belousov

Department of Embryology, Faculty of Biology, Lomonosov Moscow State University, Moscow 119991, Russia

ARTICLE INFO

Article history:

Received 24 September 2011

Received in revised form

31 January 2012

Accepted 2 February 2012

Available online 11 February 2012

Keywords:

Epithelial folding

Mechanically induced cell shape changes

Endocytosis

Xenopus laevis

ABSTRACT

Although the folding of epithelial layers is one of the most common morphogenetic events, the underlying mechanisms of this process are still poorly understood. We aimed to determine whether an artificial bending of an embryonic cell sheet, which normally remains flat, is reinforced and stabilized by intrinsic cell transformations. We observed both reinforcement and stabilization in double explants of blastocoel roof tissue from *Xenopus* early gastrula embryos. The reinforcement of artificial bending occurred over the course of a few hours and was driven by the gradual apical constriction and radial elongation of previously compressed cells situated at the bending arch of the concave layer of explant. Apical constriction was associated with actomyosin contraction and endocytosis-mediated engulfing of the apical cell membranes. Cooperative apical constrictions of the concave layer of cells produced a tensile force that extended over the entire surface of the explant and correlated with apical contraction of the concave side cells. In the explants taken from the anterior regions of the embryo, this reinforcement was more stable and the bending better expressed than in those taken from suprablastoporal areas. The morphogenetic role of cell responses to the bending force is discussed.

© 2012 Elsevier Ireland Ltd. All rights reserved.

1. Introduction

The folding of epithelial layers is one of the most common and precisely regulated modes of morphogenesis throughout the animal kingdom. This folding is a dominant means of molding the specific shapes of organisms and has been described by classical embryologists in great detail; however, the motive forces and, in particular, the spatiotemporal control of the folding patterns are still poorly understood. Studies of epithelial folding are not only of fundamental interest but also are important in bioengineering and regenerative medicine research (Davidson et al., 2010; Zartman and Shvartsman, 2010). Concerning motive forces, in a number of cases, the formation of a fold was found to be mediated by the apical constriction and radial elongation of cells located at the con-

cave side of the fold. This response is attributed to the coordinated work of the cytoskeleton (actin and microtubules) and the motor protein Myosin II (Lee and Harland, 2007; Martin et al., 2010). Several different proteins regulate actin contractility, including Shroom3 (Haigo et al., 2003) and Lulu (Nakajima and Tanoue, 2010). However, it is unclear whether there are any universal mechanisms of epithelial folding. For example, apical constriction in the neural plate of chick embryos (Schoenwolf et al., 1988) and other mammals (Ybot-Gonzalez and Copp, 1999) can occur when microfilaments are disrupted. Another unsolved problem relates to the spatiotemporal regulation of folding patterns. Several models have been suggested to explain the location and arrangement of folds under the influence of either diffusing substances or mechanical stresses. The latter class of models, which was

^{*} Corresponding author. Tel.: +7 495 939 3915; fax: +7 495 939 4309.

E-mail addresses: s.kremnyov@googlemail.com (S.V. Kremnyov), tanyatros@list.ru (T.G. Troshina), morphogenesis@yandex.ru (L.V. Belousov).

0925-4773/\$ - see front matter © 2012 Elsevier Ireland Ltd. All rights reserved.

doi:10.1016/j.mod.2012.02.001

first presented by Odell et al. (1981), and other morphomechanical approaches have recently attracted increased interest (e.g., Varner et al., 2010; Martin et al., 2010; Luu et al., 2011). Several sets of data, obtained mostly from *Drosophila* embryos, suggest that mechanical forces not only drive independently established folding processes but may also act as triggering signals (Pouille et al., 2009; Fernandez-Gonzalez et al., 2009a,b; Taguchi et al., 2011). These data suggest that a mechanically based feedback circuit exists that provides self-organization of morphological patterns (Fernandez-Gonzalez et al., 2009a,b). In this paper, we demonstrate for the first time the formation of a fold from embryonic material that normally remains flat (the ventral ectoderm of *Xenopus* early gastrula embryos) by an artificially imposed compressive force. We also show that the primary response of a cell to this force is the constriction and engulfment of apical cell surfaces, which require the concerted action of endocytosis and actomyosin contractility.

2. Materials and methods

Experiments were performed on *Xenopus laevis* (Daudin) embryos obtained from hormonally stimulated adult frogs and cultured at room temperature.

2.1. Microsurgery

Before operations, embryos were de-jellied with 2.5% cysteine solution and liberated by forceps from vitelline membranes. During and after operation, embryos were cultured in 2% agarose-coated plastic Petri dishes filled with Marc's modified Ringer's (MMR) solution (100 mM NaCl, 2 mM KCl, 2 mM CaCl₂, 1 mM MgCl₂, 5 mM HEPES, pH 7.4). Experiments were performed on *X. laevis* embryos at developmental stages 10–10 1/2 (early gastrula) as described by Nieuwkoop and Faber (1956). Pieces of blastocoel roofs that were excised from homologous regions of a pair of the same stage embryos were fused by their inner surfaces, extensively bent along their mid-lines and inserted vertically into a groove dig with a knife into an agarose substrate to fix the imposed bending (Fig. 1A). The bending plane was oriented either parallel or perpendicular to the anteroposterior axis of the embryo. Because the bending orientation did not affect the obtained results, we describe these results together. We examined the bending response of sandwiches prepared from three different zones of the blastocoel roof arranged in anteroposterior succession and defined as ventral, dorsal and suprablastoporal. The bent samples were cultured for different time periods up to 24 h and then fixed for histology.

2.2. Evaluation of local tension by tissue incision

Assuming that the angles formed by recoiling tissue edges immediately after local incisions are roughly proportional to the tensions on the tissue surface (Hutson et al., 2003), we performed incisions at the bending apex and the lateral surface of the samples at different times (from 5 min to 24 h) after artificial bending. For each time point, a minimum of

five incisions were made, one incision per sample. To study the effect of bending on incision angles, we prepared unperturbed (unbent) double explants and incised them at the same time points. All samples were fixed in Bouin's fluid 30 s after incision and underwent routine histology for paraffin sectioning. The incision angles were measured on photographs of the medial sections through the incised areas.

2.3. Cytoskeletal inhibitors

All inhibitors were diluted in MMR at the following final concentrations: 1 μM latrunculin B, 10 μM cytochalasin D, 300 μM ML-7, 100 μM blebbistatin, 50 μM Y-26732, 15 μg/ml nocodazole, and 20 μg/ml taxol (Lee and Harland, 2007). One percent DMSO in MMR was used as a control solution. Each experiment was performed on six samples.

2.4. Optical histology

Samples were fixed in 2.5% glutaraldehyde, postfixed in 1% osmium tetroxide, embedded in epoxy resin (Epon-812) and examined with a Carl Zeiss microscope Axiovert 25 CFL with a Zeiss AxioCam HRc camera, in the sagittal or transverse semi-thin sections stained by 1% toluidine blue.

2.5. Transmission electron microscopy (TEM)

For TEM, Epon-embedded ultrathin sections stained with 1% uranylacetate and lead citrate were prepared and examined using a JEM-1011 microscope with a Gatan ES500W Model 782 camera.

2.6. Scanning electron microscopy (SEM)

For SEM, total and fractured samples were fixed in 2.5% glutaraldehyde, postfixed in 1% osmium tetroxide and dehydrated in ethanol and acetone. Total samples were prepared for SEM. Samples were examined with a CamScan S-2 microscope.

2.7. Confocal microscopy

Confocal microscopy was performed on a Zeiss Axiovert200m LSM 510Meta with a Zeiss AxioCam HRm camera.

2.8. Morphometric measurements

Morphometric measurements were made using ImageJ. We measured the apical indices (AI) of epithelial cells situated at the concave or convex sides of the bending arch from photographs of microscopic sections of Epon embedded samples. AI is the ratio L/W between the maximal cell length (L) in the direction perpendicular to its apical surface and cell width (W), as observed on transverse sections (Fig. 1B). Each measurement was performed on at least five normal (non-treated) samples and six samples treated with any of the cytoskeletal drugs. In each case, the measurements were made on 50 cells per sample.

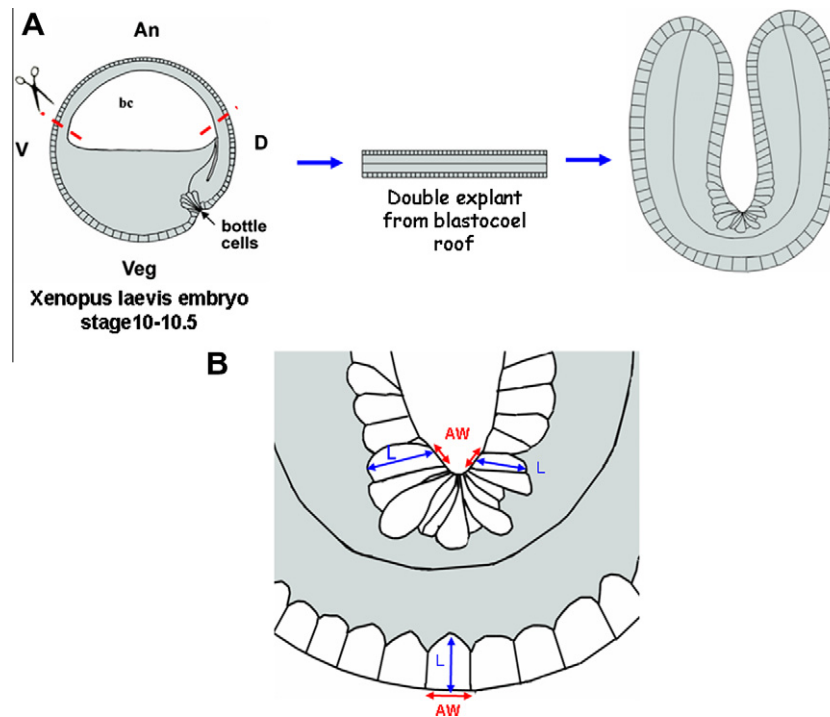


Fig. 1 – Scheme of the operation (A) and of the apical index measurements (B).

2.9. Time-lapse filming

Time-lapse filming was performed using a digital camera (DCM130) on an Olympus SZX9 stereomicroscope. The samples inserted into the grooves were filmed from above.

2.10. Statistics

Statistical significance was determined using the Statistica 6.0 program (Section Basic Statistics). We compared the AI values of concave and convex surface cells belonging to samples fixed at different times after bending, prepared from different anteroposterior regions and treated with different cytoskeletal inhibitors. In addition, we analyzed the difference between *L* and *W*. Using the same program, we determined a correlation coefficient between AI and incision angles.

3. Results

3.1. Cell movements, apical indices and morphology of bent ventral ectoderm sandwiches

Immediately after bending, the edges of the inner layer started to roll outward, tending to fuse with the outer layer edges. This rolling is also a part of the standard response of an excised tissue piece, directed towards wound closure. In a few minutes, these movements were reversed, which lasted for a few hours and were directed toward closure of the bending slit (Fig. 2A–C and Supplement). Both the bending and slit-closing movements correlated with an increase in the apical indices of concave, side, outer ectodermal cells situated at the fold arch (Fig. 3). An initial AI increase was detected as

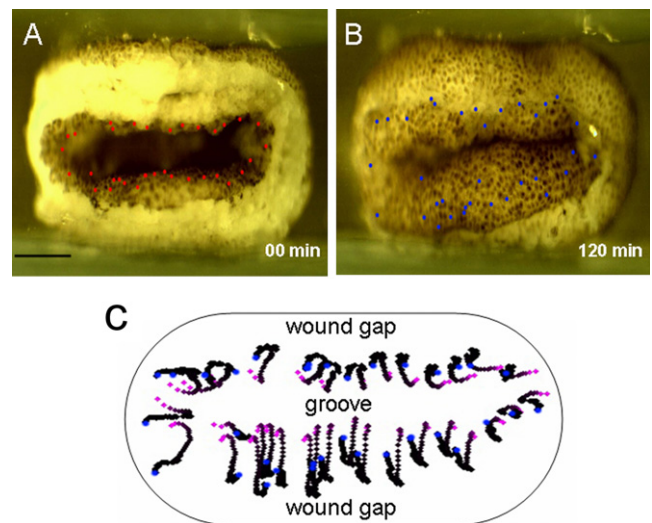


Fig. 2 – Two frames from a time-lapse film (A and B) and a diagram of cell trajectories (C) covering the first two hours after bending a sandwich, prepared from the ventral ectoderm. Pink points: starting positions of a set of cells, belonging to the inner sandwich layer; blue points: final positions of the same cells. As observed in C, the inner layer cells initially move outwards to close the wound gap and subsequently become involved in an opposing movement that closes the slit of the bent sample.

soon as 2 min after the end of the bending procedure. Within this brief time period, the apical surfaces of the concave side cells were rounded and did not show any signs of reduction (Fig. 3A). Therefore, we regarded these deformations as a purely passive response to compression. Further AI increase

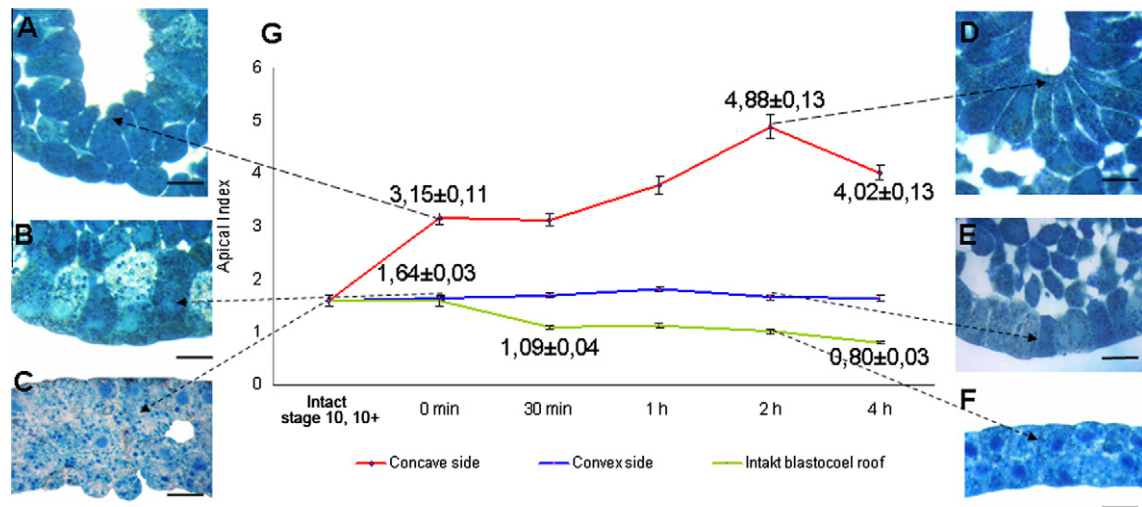


Fig. 3 – Dynamics of the apical indexes (AI) of the outer ectodermal cells situated at the concave and convex sides of the bent sandwiches compared to the AI of intact blastocoel roof cells. Times after bending procedure are shown. Insets illustrate the measurement areas of 2 min (left) and 2 h samples. Data represent the mean ± SE.

occurred gradually and was associated with the flattening and diminishment of apical cell surfaces (Figs. 3D, 4A). Prolonged arrays of elongated and bottle-shaped cells formed in the outer concave layer (Fig. 8, middle row). These events suggest an active cell response to mechanical compression. Such a response was in sharp contrast with the behavior of convex side cells in bent sandwiches and blastocoel roof cells of intact embryos. The convex side cells did not show any significant AI changes (Fig. 3B), while the intact blastocoel roof cells demonstrated statistically significant flattening (AI decrease) only at the end of the observed time period, which we relate to epiboly (Fig. 3G).

Immediately after artificial bending, both parts of the sandwich, particularly the outer layer, appeared disintegrated, with the outer ectodermal cells taking on rounded shapes (Fig. 5A). Within a few hours, the integrity of the outer ectodermal layer was restored, while the inner cells created a common mass that was gradually rearranged because of increasing thickness (Fig. 5B and C). From several hours onward, small cavities (homologous to the blastocoel) emerged in the internal cell mass (Fig. 5D). By 8 h, the sandwich surfaces appeared to be extensively folded (Fig. 5D and E).

3.2. Dynamics of tension on explant surfaces, as revealed by local incision

As observed in Figs. 6 and 7, the incision located at the bending apex produced a substantial gap within 5 min of bending, whereas incisions in the lateral areas reached the same value 30 min later. Therefore, the immediate result of artificial bending was a strictly localized stretching of the convex surface and the creation of a tension inequality between the convex and concave surfaces at the bending apex. The subsequent spreading of a roughly uniform tension throughout the entire external surface correlates with the fusion of the opposite layers of outer ectoderm at the edges of a progressively narrowed slit. To test whether a pulling force is produced by apical contraction of the concave side cells that could contribute to the tension on the outer surface, we determined whether there is a positive correlation between the average AI of cells located within the bending groove and the angles of incision gaps at the outer surface of the same samples (Fig. 8). We selected a group of six samples at the 4 h time point for these measurements. Despite a restricted number of samples, the correlation turned out to be signifi-

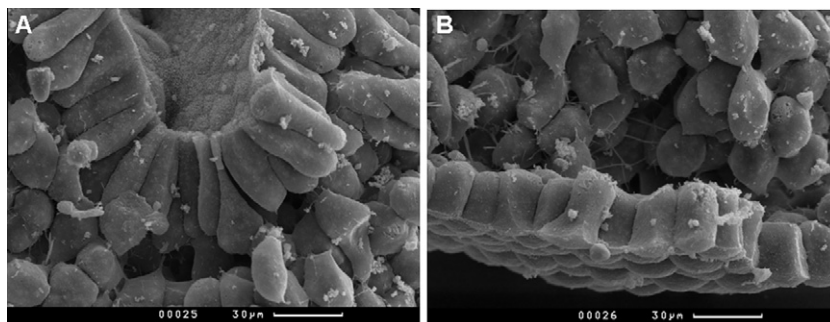


Fig. 4 – Scanning electron microscopy view of the concave (A) and convex (B) areas of the bent blastocoel roof sandwiches 2 h after operation.

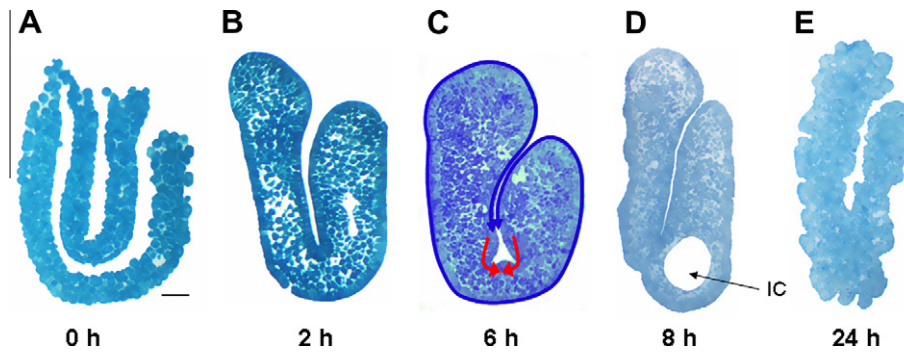


Fig. 5 – Dynamics of shape changes in the bent blastocoel roof sandwiches, as observed in the medial sections. (A) 0 h, (B) 2 h, (C) 6 h, (D) 8 h, (E) 24 h after operation. (C) displays the arrangement of active contractile forces generated by cells lining the groove (red converged arrows) and the resulting tensile stresses (blue curved arrow). IC: inflated cavities in the inner parts of tissue sandwiches.

cantly positive ($r = +0.87$). Consequently, by this time, the entire bent explant was transformed into a mechanically integrated unit with tensile forces produced by apically contracting cells spread across the entire surface. The role of bending-produced pulling forces in the increase of overall tension is also supported by our finding of significantly smaller values of incision angles, and hence tension values, in flat (i.e., unbent) explants up to the 2 h time point. A sharp increase in tension in 4 h flat explants was associated with the formation of a number of inflated cavities (IC, Fig. 5), which was typical of all ventral ectoderm samples at this time point. The near complete loss of tension in both the bent and flat 24 h samples (corresponding to the advanced neurula stage) appears to be a non-specific age phenomenon.

3.3. Role of endocytosis and cytoskeleton dynamics in the AI increase

Several studies have indicated that apical cell constriction is accompanied by endocytosis of the apical membrane (Chua et al., 2009; Lee and Harland, 2010). To detect whether endocytosis occurred in our samples, we added the vital lipophilic dye FM 4-64FX to 1.5 h bent explants and cultured them for 30 min. At this point, the AI difference between concave and convex side epithelial cells have reached its maximal value. We observed that dye absorption in concave side cells exceeded the absorption in the convex side cells, suggesting that extensive endocytosis occurs in concave side cells (Fig. 9A). We additionally observed a large number of vesicles in subapical parts of the concave side cells and numerous outgrowths on their apical membranes, which was not observed in the convex side cells (Fig. 9, cf B–E).

All the cytoskeletal drugs used significantly inhibited the AI increase of concave side cells without noticeably affecting the convex side cells. Inhibition was mostly due to the suppression of apical constriction rather than the suppression of radial elongation (Fig. 10, cf A–C). The most pronounced effects were generated by ML-7 or blebbistatin treatment, both of which are known to decouple acto-myosin interactions. Less pronounced defects were observed after treatment with cytochalasin D or with inhibitors of microtubules assembly (nocodazole and taxol).

3.4. Regional differences in active responses to bending

Although samples prepared from all regions of the blastocoel roof demonstrated an AI increase in the concave side cells situated at the bending arch, the amount of this increase gradually diminished in the anteroposterior direction (Fig. 11B). This diminishment was due to a reduction in radial cell lengths, as the amount of apical constriction remained constant (Fig. 11C and D). The sandwiches prepared from posterior regions showed a greater tendency to unbend by crawling out of the slit. After 2 h of incubation, approximately one half of the bent sandwiches prepared from the SBA (suprablastoporal area) moved out of the slit and straightened; in the remaining explants, the imposed curvature was considerably reduced. Most of these samples initiated elongation in the anteroposterior direction after 2 h, and the imposed fold stayed flattened. In the ventral samples, the imposed bending was retained in 80% of the cases after 4 h of cultivation and in 30% after 24 h. By our observations, unbending in the resting cases was due to the turgor pressure in newly arisen fragments of the blastocoel cavity.

4. Discussion

The main result reported in this paper is that the blastocoel roof cells from early gastrula *Xenopus* embryos actively react to mechanical compressions produced by an applied force by gradually undergoing apical constriction and radial elongation movements. This response occurs in a cooperative way, as more or less prolonged arrays of elongated cells are formed. This process increases tension on the surface of the entire explant and produces a macromorphological result, namely, the reinforcement and stabilization of an imposed fold that is ectopic to this embryonic area during normal development. Reinforcement can be interpreted in terms of the hyper-restoration (HR) model of morphogenesis (Belousov et al., 2006), which claims that an embryonic cell or tissue affected by an external stretching or compressive mechanical force develops an active response directed toward diminishing the imposed stress. Several examples of this response have been described, such as in cells responding to artificial stretching by generating internal pressure forces in the direc-

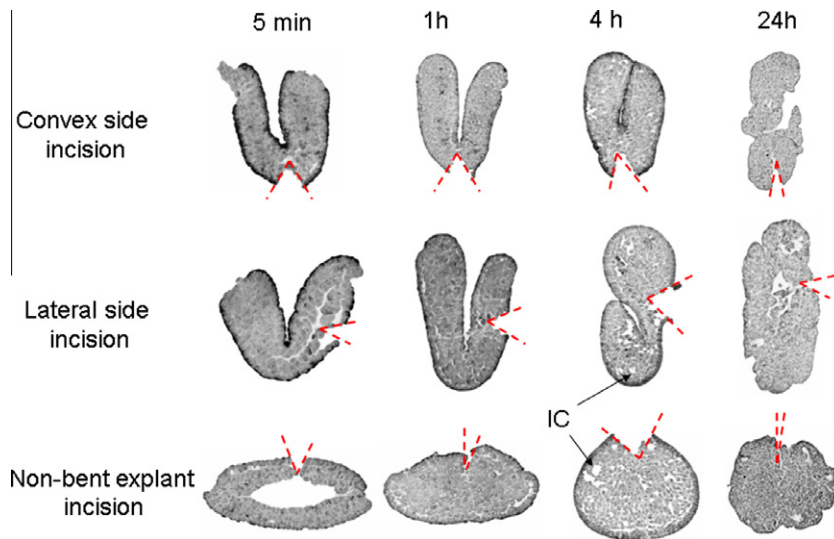


Fig. 6 – Incisions gaps as observed in the medial sections of the samples fixed 30 s after operations. Upper row: incisions at the bending apices of the bent explants; middle row: incisions at the lateral surfaces of bent explants; lower row: incisions on the surface of flat (unbent) double explants. Times of incubation are shown. Dashed lines display the gap angles. IC: inflated cavities.

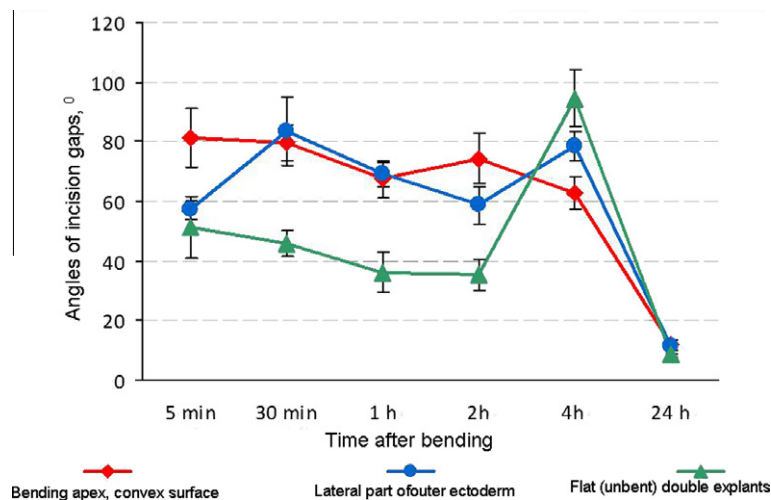


Fig. 7 – Temporal dynamics of incision gap angles at the bending apex (red), in the outer lateral ectoderm (blue) of bent explants and in the flat (unbent) explants (green). Data represent the mean \pm S.

tion of stretch (Belousov et al., 2006; Troshina and Belousov, 2009). In this study, we provide the first clear example of an HR response to cell compression, namely the production of tension. The cellular response to compression is confirmed first by its gradualness, as the response lasts several hours, and second by its sensitivity to different cytoskeletal drugs. Among the latter, the most pronounced effects were observed with ML-7 and blebbistatin, indicating a crucial role for actomyosin contractility in the response to compression. Two other main components of the response were endocytosis and the subsequent engulfment of the apical cell membrane, as revealed by the use of a specific marker and transmission electron microscopy (Fig. 7). Both components seem to be tightly coupled with each other, as the decreasing tension in the apical cell membrane caused by its shrinkage due to actomyosin contractility can directly stimulate endocytosis (Apodaca, 2002).

Previous studies have demonstrated the involvement of endocytosis in normal and relaxation-associated morphogenetic processes (Betchaku and Trinkaus, 1986; Ivanenkov et al., 1990).

We have also measured the relation between the incision gap length and the total length of the explant outer surfaces, which can be taken as a measure of the bent explant strain. As a result, we obtained a value of approximately 15%, which is on the same order as the strain in the blastoporal circumference (24%) that is associated with normal gastrulation and was measured using the same technique (Kornikova et al., 2009). Therefore, the forces involved in active bending are within the range of those involved in normal morphogenesis.

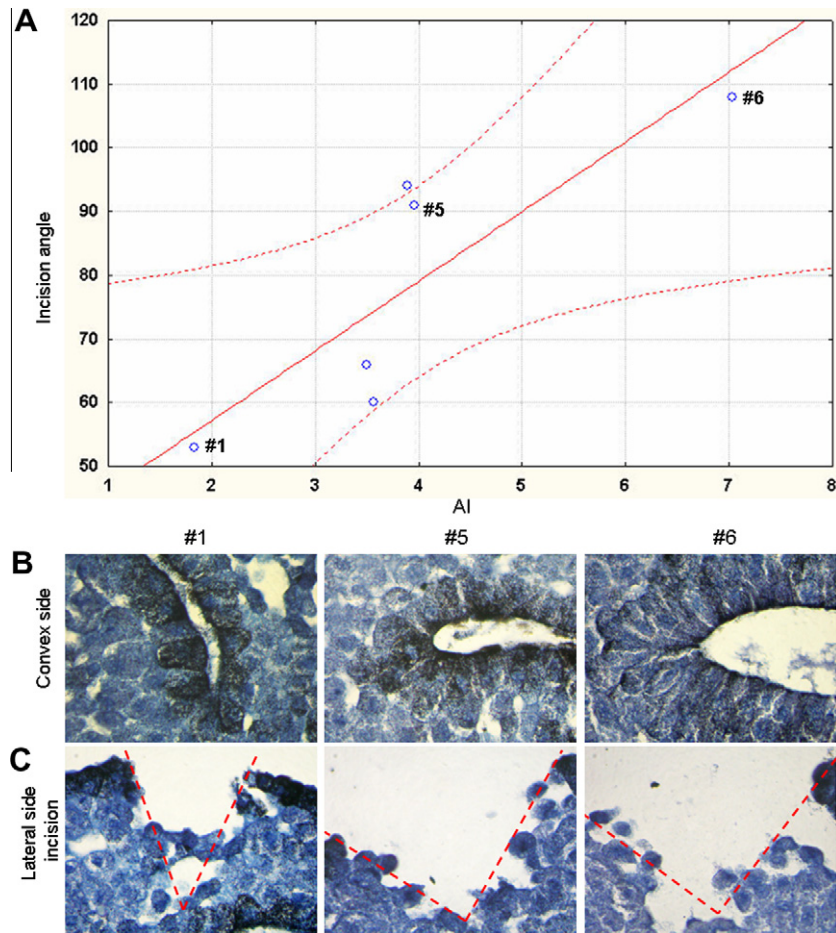


Fig. 8 – Correlations between the average apical indices and the angles of incision gaps in 4 h bent samples. (A) Correlation plot ($r = +0.85$). (B) Files of cells with increased AI from the groove regions of three different samples. (C) Incision gaps as seen from the lateral outer surfaces of the same samples.

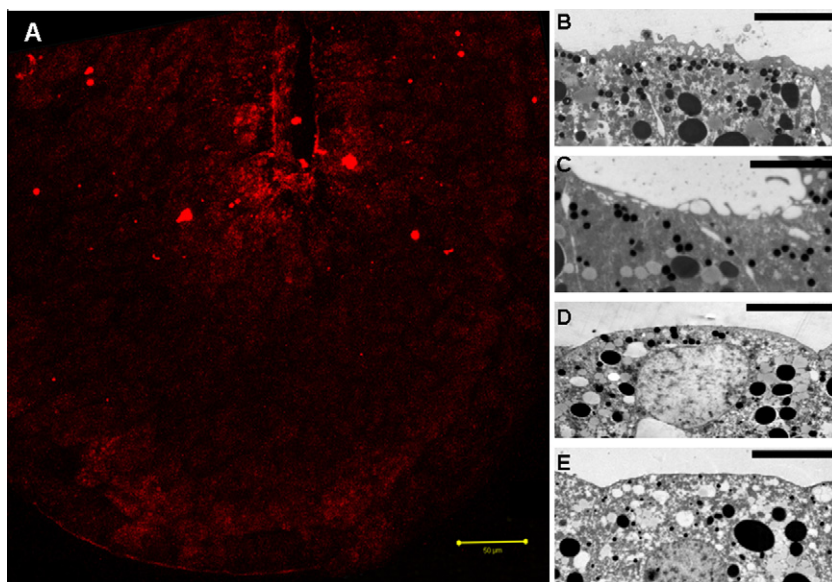


Fig. 9 – Endocytosis and surface dynamics in the tip regions of 2 h bent sandwiches. (A) Absorption of a lipophilic dye FM 4-64FX in the concave side cells is increased compared to convex side cells. (B–E) Transmission electron microscopic view of the apical surfaces of the concave (B and C) and convex (D and E) side cells. Note the extensive ruffling of the apical cell membrane in B and C.

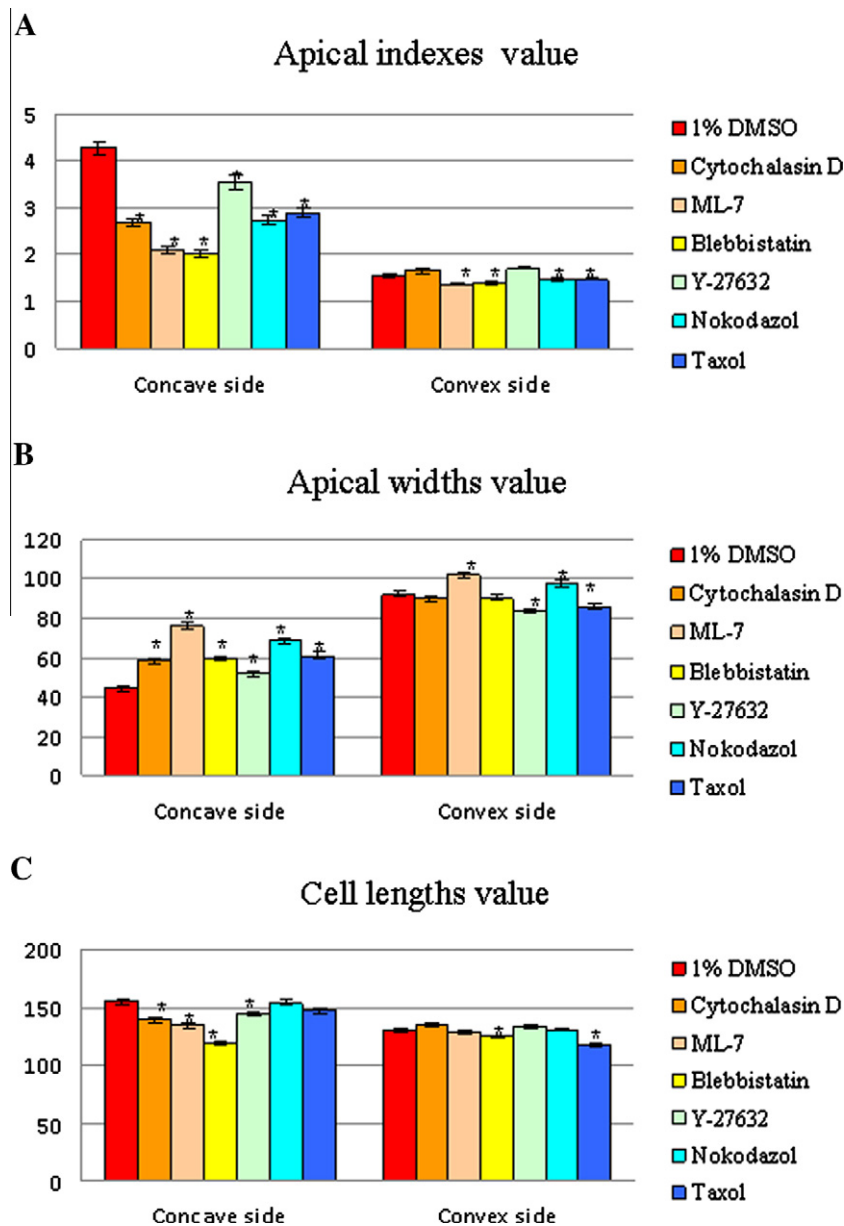


Fig. 10 – Effects of the cytoskeletal drugs (shown at right) on the (A), (B) and (C) (μm) of the concave and convex side cells from the tip regions of 2 h bent sandwiches prepared from the ventral parts of the blastocoel roof. For each set of measurements, six different samples were analyzed with 50 cells per sample. Bars indicate mean value \pm SE.

A peculiar and unexpected result of our experiments was that the effect of bending on tissues located in the blastopore vicinity was less pronounced and highly reversible compared to ventrally located tissues (Fig. 11). In subsequent developmental stages, the suprablastoporal area (SBA) generates the neural fold; therefore, the bending response could be expected to be mechanically induced much easier within the SBA than in tissues that do not typically participate in these deformations. The observed result indicates the opposite and suggests that SBA tissues, unlike ventral tissue, are strictly programmed to perform morphogenetic movements according to a precise spatiotemporal schedule and are capable of resisting interventions that would violate this pattern. As shown by Troshina and coauthors (2011), it is much more

difficult to change the direction of cell intercalation in SBA tissues by abnormally oriented stretching than it is to change the direction of ventral tissue cell behavior.

Therefore, we conclude that the artificial fold can best be reproduced on embryonic material, which, in normal development, is not affected by any of the forces that can trigger folding; this is the case for the ventral ectoderm of the early gastrula *Xenopus* embryo. It is important to know whether the fold-triggering situation reproduced in our experiments is used in normal development. To that end, a recent morphomechanical study analyzed the formation of the head fold in the early chicken embryo (Varner et al., 2010). The first step in head fold formation is a planar longitudinal compression of a flat cell sheet, where the compression is generated by

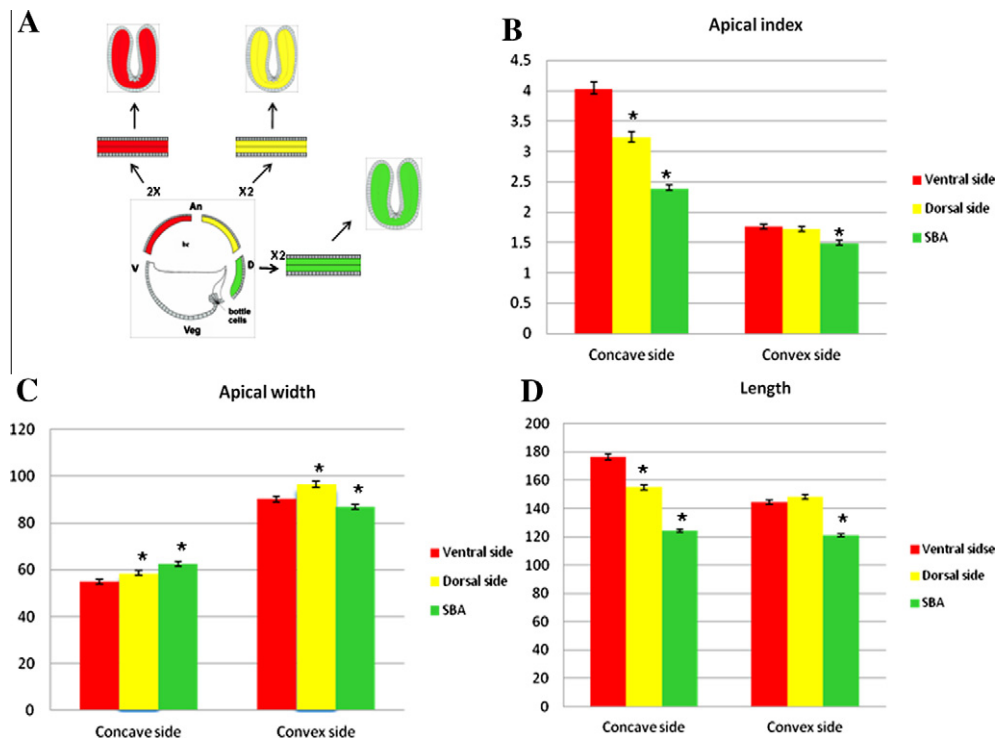


Fig. 11 – Anteroposterior regional differences in the bending responses along the blastocoel roof of *Xenopus* embryos. (A) schemes of operations. (B–D) diagrams of the apical indices, apical widths and radial lengths of the concave and convex side outer ectodermal cells from the tip regions of 2 h samples. The regional AI differences are mostly related to radial cell elongation than to apical constrictions. Each region was represented by 10 different samples, 50 cells per sample. Bars indicate mean value \pm SE.

convergent extension of the anterior neural plate. This longitudinal compression is homologous to the artificial forces used in our study. The second step in head fold formation is the emergence of wedge-shaped cells on the concave surface of the fold tip, which is comparable to our findings on the concave surface of the *Xenopus* explant artificial folds. By studying both the subsequent folding of Amniota embryo blastoderms and the different types of extensively folded epithelia of meso- and endodermal origin, similar mechanisms of mechanical reinforcement can be revealed.

Acknowledgements

We thank Dr. Thierry Galli for his advices as concerning the technique of endocytosis examination. This investigation was supported by the Carl Zeiss Firm Grant “Grant for young researchers of the leading Universities of Russia”, the Russian Science Support Foundation, grant for young researchers “The best postgraduate students of Russian Academy of Sciences” and Russian Fund of Fundamental Investigations (RFFI), Grant Number 11-04-01718.

Appendix A. Supplementary data

Supplementary data associated with this article can be found, in the online version, at doi:10.1016/j.mod.2012.02.001.

REFERENCES

- Apodaca, G., 2002. Modulation of membrane traffic by mechanical stimuli. *Am. J. Physiol. Renal Physiol.* 282, F179–F190.
- Belousov, L.V., Luchinskaya, N.N., Ermakov, A.S., Glagoleva, N.S., 2006. Gastrulation in amphibian embryos, regarded as succession of biomechanical feedback events. *Int. J. Dev. Biol.* 50, 113–122.
- Betchaku, T., Trinkaus, J.P., 1986. Programmed endocytosis during epiboly of *Fundulus heteroclitus*. *Am. Zool.* 26, 193–199.
- Chua, J., Rikhy, R., Lippincott-Schwartz, J., 2009. Dynamin 2 orchestrates the global actomyosin cytoskeleton for epithelial maintenance and apical constriction. *PNAS* 106, 20770–20775.
- Davidson, L.A., Joshi, S.D., Kim, H.Y., von Dassow, M., Lin, Zhand., Shou, J., 2010. Emergent morphogenesis: elastic mechanics of a self-deforming tissue. *J. Biomech.* 43, 63–70.
- Fernandez-Gonzalez, R., Zallen, J.A., 2009a. Cell mechanics and feedback regulation of actomyosin networks. *Sci. Signal.* 101, 78.
- Fernandez-Gonzalez, R., Simoes, M., Roper, J.C., Eaton, S., Zallen, J.A., 2009a. Myosin II dynamics are regulated by tension in intercalating cells. *Dev. Cell.* 17, 736–743.
- Haigo, S.L., Hilderbrand, J.D., Harland, R.M., Wallingford, J.B., 2003. Shroom induces apical constriction and is required for hinge-point formation during neural tube closure. *Cur. Biol.* 13, 2125–2137.
- Hutson, M.S., Tokutake, Y., Chang, M.-S., Bloor, J.W., Venakides, S., Kiehart, D.P., Edwards, G.S., 2003. Forces for morphogenesis investigated with laser microsurgery and quantitative modeling. *Science* 300, 145–149.

- Ivanenkov, V.V., Meshcheryakov, V.N., Martynova, L.E., 1990. Surface polarization in loach eggs and two-cells embryos: correlation between surface relief, endocytosis and cortex contractility. *Int. J. Dev. Biol.* 34, 337–349.
- Kornikova, E.S., Korvin-pavlovskaya, E.G., Belousov, L.V., 2009. Relocations of cell convergence sites and formation of pharyngula-like shapes in mechanically relaxed *Xenopus* embryos. *Dev. Genes. Evol.* 219, 1–10.
- Lee, J.-Y., Harland, R., 2007. Actomyosin contractility and microtubules drive apical constriction in *Xenopus* bottle cells. *Dev. Biol.* 311, 40–52.
- Lee, J.-Y., Harland, R., 2010. Endocytosis is required for efficient apical constriction during *Xenopus* gastrulation. *Curr. Biol.* 20, 253–258.
- Luu, O., David, R., Ninomiya, H., Winklbaauer, R., 2011. Large-scale mechanical properties of *Xenopus* embryonic epithelium. *PNAS* 108, 4000–4005.
- Martin, A.C., Gelbart, M., Fernandez-Gonzalez, R., Kaschube, M., Wieschaus, E.F., 2010. Integration of contractile forces during tissue invagination. *J. Cell Biol.* 188, 735–749.
- Nakajima, H., Tanoue, T., 2010. Epithelial cell shape is regulated by Lulu proteins via myosin-II. *J. Cell Sci.* 123, 555–566.
- Nieuwkoop, P.D., Faber, J., 1956. *Normal Table of Xenopus laevis* (Daudin). North-Holland Publications, Amsterdam.
- Odell, G.M., Oster, G., Alberch, P., Burnside, B., 1981. The mechanical basis of morphogenesis. I. Epithelial folding and invagination. *Dev. Biol.* 85, 446–462.
- Pouille P-A., Ahmadi P., Brunet A.-Chr., Farge E., 2009. Mechanical signals trigger myosin II redistribution and mesoderm invagination in *Drosophila* embryos. *Sci Signal.* 2, ra16.
- Schoenwolf, G.C., Folsom, D., Moe, A., 1988. A reexamination of the role of microfilaments in neurulation in the chick embryo. *Anat. Rec.* 220, 87–102.
- Taguchi, K., Ishiuchi, T., Takeichi, M., 2011. Mechanosensitive EPLIN-dependent remodeling of adherens junctions regulates epithelial reshaping. *J. Cell Biol.* 194, 643–656.
- Troshina, T.G., Belousov, L.V., 2009. Mechanodependent cell movements in the axial rudiments of *Xenopus gastrulae*. *Russ. J. Dev. Biol.* 40, 115–120.
- Troshina, T.G., Glagoleva, N.S., Belousov, L.V., 2011. Statistical study of rapid mechanodependent cell movements in deformed explants of *Xenopus* embryonic tissues. *Ontogeny* 42, 346–356.
- Varner, V.D., Voronov, D.A., Taber, L.A., 2010. Mechanics of head fold formation: investigating tissue-level forces during early development. *Development* 137, 3801–3811.
- Ybot-Gonzalez, P., Copp, A., 1999. Bending of the neural plate during mouse spinal neurulation is independent of actin microfilaments. *Dev. Dyn.* 215, 273–283.
- Zartman, J.J., Shvartsman, S.V., 2010. Unit operations of tissue development: epithelial folding. *Ann. Rev. Chem. Biomol. Eng.* 1, 231–246.